Title: Oxygen intrusions sustain aerobic nitrite-oxidizing bacteria in anoxic marine zones

Authors: Pearse J. Buchanan[1,2]*, Xin Sun[1], JL Weissman[3,4], Daniel McCoy[1,5], Daniele Bianchi[5], Emily Zakem[1]

Affiliations:

[1]Department of Global Ecology, Carnegie Institution for Science; 260 Panama Street, Stanford, 94305, USA.

[2]CSIRO Environment; 3-4 Castray Esplanade, Hobart, 7004, Australia.

[3]Department of Biology, The City College of New York; 160 Convent Ave, NY, 10031, USA.

[4]Department of Marine and Environmental Biology, The University of Southern California; 3616 Trousdale Ave, Los Angeles, CA, 90089, USA.

[5]Department of Atmospheric and Oceanic Sciences, University of California Los Angeles; Los Angeles, CA, USA.

*Corresponding author. Email: pearse.buchanan@csiro.au

Abstract: Anaerobic metabolisms are thought to dominate nitrogen cycling in anoxic marine zones (AMZs). However, thriving populations of aerobic nitrite-oxidizing bacteria (NOB) in AMZs challenge this assumption and remain unexplained. Using theory and modelling, we show how periodic oxygen intrusions sustain aerobic NOB in AMZs alongside more competitive aerobic heterotrophs. Ecological theory, supported by genomics and numerical simulations, frames NOB as opportunists exploiting a fleeting supply of oxygen. Consistent with *in situ* observations, we show that simulated NOB contribute substantially (>40%) to oxygen consumption at AMZ boundaries, which implies that NOB may provide a unique stabilizing feedback to AMZs. Fine-scale ocean currents increase the metabolic diversity in AMZs, which could stabilize AMZ volume under climate change.

One-Sentence Summary: Fleeting whiffs of oxygen to the ocean's anoxic zones increase microbial diversity and alter biogeochemical cycling.

Main Text: Anoxic marine zones (AMZs) form in the Eastern Pacific and Northern Indian Oceans where consumption of oxygen by respiring aerobic organisms exceeds oxygen supply. Anoxia generates a niche for anaerobic metabolisms central to nitrogen cycling and ocean-climate feedbacks. Anaerobic metabolisms remove bioavailable nitrogen, which proximally limits ocean primary productivity over half the ocean (*1*), and produce nitrous oxide (N_2O), a potent greenhouse gas and ozone depleter (*2*). As marine deoxygenation intensifies (*3*), AMZs and nitrogen loss may expand (*4*). However, our understanding of the biogeochemical consequences of this expansion remains limited, in part because recent observations have revealed significant rates of aerobic as well as anaerobic metabolisms in AMZs (*5–10*).

How AMZs respond to ocean deoxygenation is impacted by complex and poorly understood microbial ecology. It remains unclear how anaerobic denitrification ($NO_3^- \rightarrow NO_2^- \rightarrow NO \rightarrow N_2O \rightarrow N_2$) and anammox ($NH_4^+ + NO_2^- \rightarrow N_2$), which remove bioavailable nitrogen, co-occur alongside the aerobic metabolisms of ammonia oxidation ($NH_3 + O_2 \rightarrow NO_2^-$) and nitrite oxidation ($NO_2^- + O_2 \rightarrow NO_3^-$), the two steps of chemoautotrophic nitrification that remove oxygen (*9–13*). Nitrite-oxidizing bacteria (NOB), in contrast to ammonia-oxidizing archaea (AOA), thrive in AMZs, displaying remarkably high biomass and activity in apparently anoxic waters (*12, 14–18*). The success of NOB in AMZs likely alters the rates of nitrogen loss and N_2O production (*8, 10, 19*), although the mechanism by which this occurs is not yet clear. More fundamentally, the success of aerobic NOB in AMZs challenges our understanding of how diverse aerobic and anaerobic metabolisms coexist.

Multiple explanations for nitrification in AMZs have been proposed (*20*). The high oxygen affinities of both AOA and NOB suggest that these microbes can survive at nanomolar oxygen concentrations (*8, 19*), although these chemoautotrophs are unlikely to outcompete facultatively aerobic heterotrophs for oxygen (*21*). Alternatively, certain clades of NOB and AOA may have evolved nitrite oxidation pathways using electron acceptors other than oxygen (*11, 12, 20, 22*). Others suggest that episodic oxygen supply to anoxic waters might be sufficient to sustain viable populations of nitrifiers (*8, 9, 23*). While these hypotheses are not mutually exclusive, a sufficient explanation must also illuminate why AOA exhibit relatively low abundance and activity compared with thriving NOB (*5, 15*). Here, using ecological theory and modeling, we show that fleeting oxygen intrusions can explain the observations of active, thriving aerobic NOB in AMZs.

Results

Heterotrophs exclude aerobic nitrifiers in steady-state anoxia

A leading explanation for aerobic NOB within AMZs is their high affinity for oxygen (*8, 19*). Previous theory has shown that aerobic and anaerobic metabolisms can coexist under steady-state anoxia with a cryptic oxygen supply, consistent with observations (*6, 7, 21*). However, chemoautotrophic nitrification demands significantly more oxygen than aerobic heterotrophy (*24, 25*). Consequently, aerobic nitrifiers are thought to be outcompeted by aerobic heterotrophs when oxygen is limiting (*21*).

We expanded the previous analysis (*21*) to assess the competitive outcomes of populations of the major microbial functional types within a virtual chemostat model representative of AMZ conditions (Fig. 1a; Methods). We incorporated a wider diversity of traits, accounting for differences in cell size, carbon quota, stoichiometry, maximum growth rate, biomass yields and

nutrient affinities (Tables S1 and S2). We solved for the steady-state solutions across different ratios of oxygen and organic matter supply to generate an anoxic-oxic landscape (Fig. 1b).

Despite the diversity of traits considered, both nitrifying functional types (AOA and NOB) are consistently competitively excluded by facultatively aerobic heterotrophs when oxygen is limiting (Fig. 1c). The high affinity of AOA and NOB for oxygen (*8*, *9*, *19*) does enable growth at nanomolar oxygen concentrations (*10*, *16*, *17*) (Table S3), but heterotrophs in general are the superior competitors across the plausible trait-space because they have a lower oxygen demand for biomass synthesis (Supplementary Text; Fig. S1). The point at which heterotrophy transitions to perform anaerobic metabolism (i.e., denitrification) occurs at oxygen concentrations that are less than the subsistence oxygen concentration required by AOA and NOB (Table S3). When considering the enormous diversity of heterotrophic bacteria, we expect that nitrifiers could outcompete a subset of inefficient aerobic heterotrophs for oxygen, but that other more efficient heterotrophs will consistently exclude nitrifiers when oxygen is limiting, at least under steady-state conditions.

Aerobic nitrifiers viable with oxygen intrusions to AMZs

The steady state can be considered as the climatological state of AMZs, set by the large-scale balance of physical supply and biological demand of oxygen. However, variability from fine-scale ocean currents sets the "weather" of the AMZs (*26*). These currents lead to time-varying intrusions of oxygen (*27*). Phytoplankton in shallow AMZ waters may also supply oxygen locally (*6*). This oxygen supply results in "cryptic" oxygen cycling, inferred from nanomolar oxygen concentrations (*28–30*) alongside non-zero oxygen consumption rates (*7*, *9*). We investigate how time-varying oxygen supply may allow NOB to thrive.

$$\frac{dB}{dt} = (\mu - L)B \qquad 1$$

We model the biomass (B) of a microbial population as

where the growth rate (μ) must balance the loss rate (L) for the population to be viable. In a time-varying environment, this balance can be achieved over time. Assuming that nitrifiers (AOA or NOB) are obligately aerobic, and neglecting limitation by micronutrients like iron (*31*), we consider oxygen intrusions to cause nitrifiers to switch from oxygen-limited growth (μ_{O_2}) to nitrogen-limited growth (μ_N) (Fig. 2a).

Following Litchman & Klausmier (*32*), we estimate the fraction of time, f, that nitrifiers must be released from oxygen-limited growth to sustain themselves in a low-oxygen environment (see derivation in the methods) as

$$f = \frac{L - \mu_{O_2}}{\mu_N - \mu_{O_2}} \qquad 2$$

where μ_{O_2} and μ_N are the oxygen- and nitrogen-limited growth rates (day^{-1}), respectively, and L is the loss rate (day^{-1}), which in the environment represents the integrated loss to predators, viral lysis, cell maintenance, and other mortality.

To simplify, we can assume μ_{O_2} is negligible when oxygen is inaccessible (ignoring potential anaerobic metabolism (*11, 12, 20*)). Also, if the nitrogen resource (nitrite for NOB or ammonium for AOA) is abundant, then μ_N may approach the maximum growth rate (μ^{max}). With both assumptions,

$$f \approx \frac{L}{\mu^{max}}, \qquad 3$$

and the fraction of time that oxygen does not limit growth is approximated by the ratio of the population's loss rate to maximum growth rate. If $L \ll \mu^{max}$, f approaches zero, implying viability in environments with infrequent oxygen intrusions.

This theory can explain the divergent activities of NOB and AOA in AMZs. It is typical for nitrite to accumulate and for ammonium to be depleted in AMZs (*12, 23*). This difference in resource availability means that during an oxygen intrusion AOA cannot maximize growth ($\mu_N < \mu^{max}$) and require more frequent oxygen intrusions to sustain a viable population (Fig. S2). Meanwhile, NOB may grow rapidly on the abundant nitrite pool.

Gene-based maximum growth rates support theory

This theory implies that the NOB inhabiting AMZs (*19, 33*) survive due to an opportunistic "boom-and-bust" life-history strategy (*32*), predominantly growing only when oxygen is available. Furthermore, Equation 3 suggests that NOB are more fit in anoxic environments when their maximum growth rates (μ^{max}) are higher. Thus, NOB may be subject to an evolutionary-scale optimization for faster growth to facilitate colonization deeper into AMZs where oxygen intrusions are rarer (*34*).

As a first test of this hypothesis, we employed a published method of using codon usage bias statistics (*35*) to estimate μ^{max} from available metagenome-assembled genomes (MAGs) of marine NOB and other functional types (Table S4). Results show higher μ^{max} for NOB than AOA and heterotrophic bacteria (*Pelagibacter spp.*) from AMZs (Fig. 2), with a wide range of μ^{max} values for NOB across AMZ and oxygenated environments. While much uncertainty lies in these estimates, a previous clustering analysis (*35*) indicates where μ^{max} estimates become more reliable, which also indicates where organisms may be categorized as a faster-growing copiotrophs (i.e., opportunists) rather than a slower-growing oligotrophs. This threshold is temperature-insensitive, unlike the 5-hour doubling time threshold presented in Weissman et al. (*35*). Many NOB μ^{max} estimates appear near or above this threshold (black dashed line in Fig. 2), suggesting that many NOB populations may indeed be considered copiotrophs.

Despite the uncertainties, this analysis supports our model-generated hypothesis that opportunistic traits would benefit NOB clades in AMZs. However, our main result – that periodic oxygen intrusions explain the success of NOB within AMZs – is not contingent on NOB having a high μ^{max} relative to other aerobic types. (Model results are qualitatively robust to variations in μ^{max}; Fig. S3). Future work should examine if similar "boom-and-bust" dynamics apply to other NOB populations in the oxygenated ocean, as suggested by the μ^{max} estimates (Fig. 2).

Chemostat simulations with oxygen intrusions support theory

Next, we applied pulses of oxygen to the virtual chemostat model to examine whether the theory is borne out when considering the AMZ microbial ecosystem (Fig. 1a). Oxygen pulses consisted of inputs ($O_{2,in}$ in Eqn. 14) ranging from 0 to 1 μM in magnitude and from 5 times per day to once every 10 days in frequency. We applied these pulses to background conditions (i.e., constant low supply rates of organic matter and oxygen) that generated deep anoxia and excluded nitrifiers under steady state (Methods; red stars in Fig. 1). Following an oxygen pulse, most experiments returned to anoxia, containing ≈10 nM of oxygen when averaged in time (Fig. 3b), roughly matching the subsistence oxygen concentration required to sustain a viable population of NOB (Table S3). Even large oxygen pulses were rapidly consumed by the microbial community, returning the system to long periods of oxygen scarcity beneath 10 nM (Fig. S4).

As predicted, the episodic pulses sustained a population of obligately aerobic NOB. Mean nitrite oxidation rates were substantially larger under anoxic regimes with fleeting oxygenation, reaching values as high as 500 nM day^{-1}, than under fully oxic or fully anoxic regimes (Fig. 3c). Peak NOB activity and biomass therefore co-occured with f values close to the analytically derived f of Eqn. 3 (dashed black line in Fig. 3b-e), indicating that coexistence of aerobic NOB with anaerobic metabolisms was beneficial. In this case, f is an emergent property of the model (Fig. 3d), calculated as the time-averaged growth limitation by oxygen (0) or nitrogen (1). f near zero indicates consistently anoxic experiments with oxygen limitation, while f near one indicates fully oxygenated experiments with nitrogen limitation caused by an absence of heterotrophic nitrate reduction. Thus, transient oxygenation of anoxic regimes maximized supply of both resources (Fig. 3e). Results were qualitatively robust across widely varying values for the maximum growth rate (μ^{max}) and other traits of NOB and other microbial functional types (Fig. S3). As Eqn. 3 suggests, lower μ^{max} for NOB increased the required frequency or strength of the oxygen intrusions required to sustain the population, shifting f to higher values. Meanwhile, aerobic AOA was sustained at minimal rates due to competition for a limited supply of both ammonium and oxygen (Fig. S5).

Nitrite oxidizers in a 3-D model AMZ

We next investigate whether NOB thrive in AMZs with realistic ocean dynamics, where mesoscale eddies supply oxygen variably over space and time. We incorporated our microbial modelling framework into an eddy-resolving, three-dimensional model of the Eastern Tropical South Pacific, which contains one of the major AMZs of the world ocean. Specifically, we integrated the key heterotrophic and chemoautotrophic microbial populations developed in our chemostat experiments (Fig. 1a) into the Biogeochemical Elemental Cycle (BEC) model (*36*), which was coupled online to the Regional Ocean Model System (ROMS) configured at an eddy-resolving (0.1° horizontal) resolution (*37*). The model explicitly simulates the time-varying nature of oxygen intrusions within the emergent AMZ.

The model produced an AMZ offshore of the Peruvian upwelling that at its most intense was 600 meters thick. Oxygen intrusions were common at the boundaries to the AMZ and were rarer at the core (Fig. 4a). As predicted by our theoretical framework, NOB biomass and activity peaked where the supply of limiting resources, oxygen and nitrite, was maximized (Fig. 4b-d,f). This included the boundaries to the AMZ, particularly the shallow edge where high rates of nitrate reduction driven by a rich organic matter flux coincided with more frequent oxygen intrusions. As predicted, ammonia oxidation did not exhibit a similar response. It displayed a weak peak near the top of the AMZ and responded weakly to oxygen intrusions (Fig. 4c,e). As a result, the

abundance of NOB relative to AOA was greatest in the AMZ (Fig. 4d), consistent with observations (*17*). Notably, the model predicted maximum rates of nitrite oxidation exceeding 300 nM day^{-1} (Fig. 4f), consistent with peak rates measured in the southeast Pacific (*16*). We provide animations of daily mean output of key rates and tracers in the supplement.

Aerobic NOB may stabilize anoxia

Aerobic nitrite oxidation was responsible for a substantial proportion (40%) of the total oxygen consumption within the AMZ, with peak contributions near the AMZ boundary (Fig. 5a and S6). A consistent result of both the chemostat (Fig. S4 and S7) and 3-D models (Fig. S8) was that aerobic NOB showed increased biomass and activity when exposed to stronger and more frequent oxygen pulses, which returned the system to anoxia. This negative feedback to oxygen intrusions also sustains the anaerobic niche, which ensures nitrite resupply via heterotrophic nitrate reduction (Fig. 5b).

These results imply that NOB may serve a unique and critical biogeochemical role as stabilizers of AMZs. This role is unique because, unlike aerobic AOA or heterotrophs, NOB growth is not typically limited by its electron donor (nitrite) since nitrite accumulates in AMZs (*12, 23*). Microbial heterotrophic populations, instead, may not exploit an oxygen intrusion as rapidly as NOB if their growth is limited by organic matter supply, which is thought to be the case (*38*). Therefore, if changes to the ocean circulation reduce the intensity of oxygen supply (*26*), this may manifest in lower NOB biomass and activity, which in turn reduces the intensity of oxygen demand. In this way, NOB may "buffer" perturbations to AMZs and thus provide a critical feedback to ocean deoxygenation.

Outlook and implications

Ocean-going studies have identified thriving populations of putatively aerobic NOB within anoxic waters of all known major ocean AMZs (*10–13, 33*), leading to numerous hypotheses to explain this counter-intuitive phenomenon. Our theoretical framework suggests that AMZs prone to oxygen intrusions are in fact ideal habitats for aerobic NOB. A "goldilocks" zone of oxygen and nitrite supply exists for NOB at the oxic-anoxic boundary, a boundary that is greatly expanded by considering the folding effect that eddies have on AMZs (e.g., Fig. 4a). Furthermore, at the shallow edge of AMZs, NOB biomass, sustained by infrequent oxygen intrusions, could also access diurnal oxygen supply from phytoplankton growing in the anoxic secondary chlorophyll maximum (*6*). NOB's ability to rapidly exploit oxygen intrusions enables them to thrive as opportunists, where rapid blooms on an oxygen pulse offset losses during oxygen scarcity. We provide initial genomic evidence that this "boom-bust" niche has selected for opportunistic traits in NOB clades.

We have been able to explain observations of NOB activity and biomass in AMZs assuming an obligate aerobic metabolism. While growth via alternative electron acceptors (*11, 12, 20*) would be complementary, we argue that it is not essential where oxygen intrusions occur, even when rare. Anaerobic growth would, however, increase NOB viability, making nitrifiers even less reliant on oxygen intrusions (Fig. S9). Additionally, NOB may also reverse the nitrite oxidoreductase enzyme and perform heterotrophic nitrate reduction (*39–41*), generating the very nitrite they require for bursts of growth during an oxygen intrusion. These anaerobic metabolisms, if accessible, would further consolidate AMZs as optimal environments and allow colonization deeper into the AMZ core.

Considering the time-varying circulation set by mesoscale eddies is critical for understanding the presence of aerobic NOB and aerobic metabolisms in general within AMZs. For the first time, we have explicitly resolved both the mesoscale and microbial populations that drive marine nitrogen cycling within a 3-D simulated AMZ, allowing for the coexistence of aerobic NOB with anaerobic metabolisms. These *in silico* results corroborate *in situ* measurements of significant oxygen consumption by NOB (*9*), but also identify NOB as opportunistic stabilizers of anoxia, particularly at the AMZ boundaries, whose presence expands the niche for anaerobic metabolism. In this sense, NOB may in fact stimulate nitrogen loss in AMZs, a view that challenges their proposed role as suppressors (*8, 10, 19*). However, the degree to which NOB are stimulators or suppressors of nitrogen loss, and whether they alter the balance of anammox to denitrification and thereby affect N_2O fluxes, will also depend on processes not well understood or resolved in this study, such as the full suite of denitrification modularity and the role that obligately aerobic or anaerobic heterotrophic populations may play (*42*). Also, our work does not account for how competitive and syntrophic interactions are affected by particle-associated microbial heterotrophs (*43*). These are significant challenges for our growing understanding of the nitrogen cycle. What is perhaps clearer is that the small-scale ocean circulation, the "weather" of the ocean, is essential to climate change assessments of AMZ volume and its biogeochemical implications, not only because it better represents the dynamics underpinning physical oxygen supply (*26, 44*), but also the ecological dynamics governing oxygen demand.

References and Notes

1. Moore, C. M. Diagnosing oceanic nutrient deficiency. *Philosophical Transactions of the Royal Society A: Mathematical, Physical and Engineering Sciences* **374**, 20150290 (2016).
2. Ravishankara, A. R., Daniel, J. S. & Portmann, R. W. Nitrous Oxide (N2O): The Dominant Ozone-Depleting Substance Emitted in the 21st Century. *Science (1979)* **326**, 123–125 (2009).
3. Bindoff, N. L. *et al.* Changing Ocean, Marine Ecosystems, and Dependent Communities. in *IPCC Special Report on the Ocean and Cryosphere in a Changing Climate* (eds. Portner, H.-O. et al.) 447–588 (2019). doi:https://www.ipcc.ch/report/srocc/.
4. Canfield, D. E., Glazer, A. N. & Falkowski, P. G. The evolution and future of earth's nitrogen cycle. *Science (1979)* **330**, 192–196 (2010).
5. Peng, X. *et al.* Revisiting nitrification in the Eastern Tropical South Pacific: A focus on controls. *J Geophys Res Oceans* **121**, 1667–1684 (2016).
6. Garcia-Robledo, E. *et al.* Cryptic oxygen cycling in anoxic marine zones. *Proc Natl Acad Sci U S A* **114**, 8319–8324 (2017).
7. Kalvelage, T. *et al.* Aerobic Microbial Respiration In Oceanic Oxygen Minimum Zones. *PLoS One* **10**, e0133526 (2015).
8. Bristow, L. A. *et al.* Ammonium and nitrite oxidation at nanomolar oxygen concentrations in oxygen minimum zone waters. *Proceedings of the National Academy of Sciences* **113**, 10601–10606 (2016).
9. Beman, J. M. *et al.* Substantial oxygen consumption by aerobic nitrite oxidation in oceanic oxygen minimum zones. *Nat Commun* **12**, 7043 (2021).
10. Füssel, J. *et al.* Nitrite oxidation in the Namibian oxygen minimum zone. *ISME J* **6**, 1200–1209 (2012).
11. Babbin, A. R. *et al.* Multiple metabolisms constrain the anaerobic nitrite budget in the Eastern Tropical South Pacific. *Global Biogeochem Cycles* **31**, 258–271 (2017).

12. Babbin, A. R., Buchwald, C., Morel, F. M. M., Wankel, S. D. & Ward, B. B. Nitrite oxidation exceeds reduction and fixed nitrogen loss in anoxic Pacific waters. *Mar Chem* **224**, 103814 (2020).
13. Beman, J. M., Leilei Shih, J. & Popp, B. N. Nitrite oxidation in the upper water column and oxygen minimum zone of the eastern tropical North Pacific Ocean. *ISME J* **7**, 2192–2205 (2013).
14. Sun, X. & Ward, B. B. Novel metagenome-assembled genomes involved in the nitrogen cycle from a Pacific oxygen minimum zone. *ISME Communications* **1**, 26 (2021).
15. Peng, X. *et al.* Ammonia and nitrite oxidation in the Eastern Tropical North Pacific. *Global Biogeochem Cycles* **29**, 2034–2049 (2015).
16. Santoro, A. E. *et al.* Nitrification and Nitrous Oxide Production in the Offshore Waters of the Eastern Tropical South Pacific. *Global Biogeochem Cycles* **35**, 1–21 (2021).
17. Fuchsman, C. A., Devol, A. H., Saunders, J. K., McKay, C. & Rocap, G. Niche partitioning of the N cycling microbial community of an offshore oxygen deficient zone. *Front Microbiol* **8**, 1–18 (2017).
18. Evans, N., Tichota, J., Moffett, J. W. & Devol, A. H. Prolific nitrite reoxidation across the Eastern Tropical North Pacific Ocean. *Limnol Oceanogr* (2023) doi:10.1002/lno.12380.
19. Sun, X., Frey, C., Garcia-Robledo, E., Jayakumar, A. & Ward, B. B. Microbial niche differentiation explains nitrite oxidation in marine oxygen minimum zones. *ISME J* **15**, 1317–1329 (2021).
20. Sun, X., Frey, C. & Ward, B. B. Nitrite Oxidation Across the Full Oxygen Spectrum in the Ocean. *Global Biogeochem Cycles* **37**, (2023).
21. Zakem, E. J., Mahadevan, A., Lauderdale, J. M. & Follows, M. J. Stable aerobic and anaerobic coexistence in anoxic marine zones. *ISME J* **14**, 288–301 (2020).
22. Kraft, B. *et al.* Oxygen and nitrogen production by an ammonia-oxidizing archaeon. *Science (1979)* **375**, 97–100 (2022).
23. Kalvelage, T. *et al.* Nitrogen cycling driven by organic matter export in the South Pacific oxygen minimum zone. *Nat Geosci* **6**, 228–234 (2013).
24. Tilman, D., Kilham, S. S. & Kilham, P. *Phytoplankton Community Ecology: The Role of Limiting Nutrients*. *Source: Annual Review of Ecology and Systematics* vol. 13 https://www.jstor.org/stable/2097072?seq=1&cid=pdf- (1982).
25. Zakem, E. J. & Follows, M. J. A theoretical basis for a nanomolar critical oxygen concentration. *Limnol Oceanogr* **62**, 795–805 (2017).
26. Lévy, M., Resplandy, L., Palter, J. B., Couespel, D. & Lachkar, Z. The crucial contribution of mixing to present and future ocean oxygen distribution. in *Ocean Mixing* (eds. Naveira-Garabato, A. C. & Meredith, M. P.) (2021).
27. Margolskee, A., Frenzel, H., Emerson, S. & Deutsch, C. Ventilation Pathways for the North Pacific Oxygen Deficient Zone. *Global Biogeochem Cycles* **33**, 875–890 (2019).
28. Thamdrup, B., Dalsgaard, T. & Revsbech, N. P. Widespread functional anoxia in the oxygen minimum zone of the Eastern South Pacific. *Deep Sea Research Part I: Oceanographic Research Papers* **65**, 36–45 (2012).
29. Tiano, L. *et al.* Oxygen distribution and aerobic respiration in the north and south eastern tropical Pacific oxygen minimum zones. *Deep Sea Research Part I: Oceanographic Research Papers* **94**, 173–183 (2014).
30. Bristow, L. A. *et al.* N2 production rates limited by nitrite availability in the Bay of Bengal oxygen minimum zone. *Nat Geosci* **10**, 24–29 (2017).
31. Shafiee, R. T., Snow, J. T., Zhang, Q. & Rickaby, R. E. M. Iron requirements and uptake strategies of the globally abundant marine ammonia-oxidising archaeon, Nitrosopumilus maritimus SCM1. *ISME J* (2019) doi:10.1038/s41396-019-0434-8.

32. Litchman, E. & Klausmeier, C. A. Competition of Phytoplankton under Fluctuating Light. *Am Nat* **157**, 170–187 (2001).
33. Sun, X. *et al.* Uncultured Nitrospina-like species are major nitrite oxidizing bacteria in oxygen minimum zones. *ISME J* **13**, 2391–2402 (2019).
34. Kwiecinski, J. v. & Babbin, A. R. A High□Resolution Atlas of the Eastern Tropical Pacific Oxygen Deficient Zones. *Global Biogeochem Cycles* **35**, (2021).
35. Weissman, J. L., Hou, S. & Fuhrman, J. A. Estimating maximal microbial growth rates from cultures, metagenomes, and single cells via codon usage patterns. *Proceedings of the National Academy of Sciences* **118**, (2021).
36. Bayer, B., McBeain, K., Carlson, C. A. & Santoro, A. E. Carbon content, carbon fixation yield and dissolved organic carbon release from diverse marine nitrifiers. *Limnol Oceanogr* (2022) doi:10.1002/lno.12252.
37. Moore, J. K., Doney, S. C. & Lindsay, K. Upper ocean ecosystem dynamics and iron cycling in a global three-dimensional model. *Global Biogeochem Cycles* **18**, 1–21 (2004).
38. McCoy, D., Damien, P., Clements, D., Yang, S. & Bianchi, D. Pathways of Nitrous Oxide Production in the Eastern Tropical South Pacific Oxygen Minimum Zone. *Global Biogeochem Cycles* (2023) doi:10.1029/2022GB007670.
39. Babbin, A. R., Keil, R. G., Devol, A. H. & Ward, B. B. Organic Matter Stoichiometry, Flux, and Oxygen Control Nitrogen Loss in the Ocean. *Science (1979)* **344**, 406–408 (2014).
40. Lücker, S., Nowka, B., Rattei, T., Spieck, E. & Daims, H. The Genome of Nitrospina gracilis Illuminates the Metabolism and Evolution of the Major Marine Nitrite Oxidizer. *Front Microbiol* **4**, 1–19 (2013).
41. Füssel, J. *et al.* Adaptability as the key to success for the ubiquitous marine nitrite oxidizer *Nitrococcus*. *Sci Adv* **3**, (2017).
42. Chicano, T. M. *et al.* Structural and functional characterization of the intracellular filament-forming nitrite oxidoreductase multiprotein complex. *Nat Microbiol* **6**, 1129–1139 (2021).
43. Kuypers, M. M. M., Marchant, H. K. & Kartal, B. The microbial nitrogen-cycling network. *Nat Rev Microbiol* **16**, 263–276 (2018).
44. Bianchi, D., Weber, T. S., Kiko, R. & Deutsch, C. Global niche of marine anaerobic metabolisms expanded by particle microenvironments. *Nat Geosci* **11**, 263–268 (2018).
45. Busecke, J. J. M., Resplandy, L. & Dunne, J. P. The Equatorial Undercurrent and the Oxygen Minimum Zone in the Pacific. *Geophys Res Lett* **46**, 6716–6725 (2019).
46. Spieck, E., Keuter, S., Wenzel, T., Bock, E. & Ludwig, W. Characterization of a new marine nitrite oxidizing bacterium, Nitrospina watsonii sp. nov., a member of the newly proposed phylum “Nitrospinae”. *Syst Appl Microbiol* **37**, 170–176 (2014).
47. Kitzinger, K. *et al.* Single cell analyses reveal contrasting life strategies of the two main nitrifiers in the ocean. *Nat Commun* **11**, 767 (2020).
48. Bianchi, D., McCoy, D. & Yang, S. Formulation, optimization, and sensitivity of NitrOMZv1.0, a biogeochemical model of the nitrogen cycle in oceanic oxygen minimum zones. *Geosci Model Dev* **16**, 3581–3609 (2023).
49. Shchepetkin, A. F. An adaptive, Courant-number-dependent implicit scheme for vertical advection in oceanic modeling. *Ocean Model (Oxf)* **91**, 38–69 (2015).
50. Shchepetkin, A. F. & McWilliams, J. C. The regional oceanic modeling system (ROMS): a split-explicit, free-surface, topography-following-coordinate oceanic model. *Ocean Model (Oxf)* **9**, 347–404 (2005).
51. Zakem, E. J. *et al.* Controls on the relative abundances and rates of nitrifying microorganisms in the ocean. *Biogeosciences* **19**, 5401–5418 (2022).

52. Seemann, T. Prokka: rapid prokaryotic genome annotation. *Bioinformatics* **30**, 2068–2069 (2014).
53. Weissman, J. L., Peras, M., Barnum, T. P. & Fuhrman, J. A. Benchmarking Community-Wide Estimates of Growth Potential from Metagenomes Using Codon Usage Statistics. *mSystems* **7**, (2022).
54. del Giorgio, P. A. & Cole, J. J. BACTERIAL GROWTH EFFICIENCY IN NATURAL AQUATIC SYSTEMS. *Annu Rev Ecol Syst* **29**, 503–541 (1998).
55. Tsementzi, D. *et al.* SAR11 bacteria linked to ocean anoxia and nitrogen loss. *Nature* **536**, 179–183 (2016).
56. Sinsabaugh, R. L., Manzoni, S., Moorhead, D. L. & Richter, A. Carbon use efficiency of microbial communities: stoichiometry, methodology and modelling. *Ecol Lett* **16**, 930–939 (2013).
57. Smith, J. M., Chavez, F. P. & Francis, C. A. Ammonium Uptake by Phytoplankton Regulates Nitrification in the Sunlit Ocean. *PLoS One* **9**, e108173 (2014).
58. Zakem, E. J. *et al.* Ecological control of nitrite in the upper ocean. *Nat Commun* **9**, (2018).
59. Taniguchi, D., Franks, P. & Poulin, F. Planktonic biomass size spectra: an emergent property of size-dependent physiological rates, food web dynamics, and nutrient regimes. *Mar Ecol Prog Ser* **514**, 13–33 (2014).
60. Giovannoni, S. J. SAR11 Bacteria: The Most Abundant Plankton in the Oceans. *Ann Rev Mar Sci* **9**, 231–255 (2017).
61. Ratnarajah, L. *et al.* Resource Colimitation Drives Competition Between Phytoplankton and Bacteria in the Southern Ocean. *Geophys Res Lett* **48**, (2021).
62. Fourquez, M. *et al.* Microbial Competition in the Subpolar Southern Ocean: An Fe–C Co-limitation Experiment. *Front Mar Sci* **6**, (2020).
63. Lam, P. *et al.* Revising the nitrogen cycle in the Peruvian oxygen minimum zone. *Proc Natl Acad Sci U S A* **106**, 4752–4757 (2009).
64. Rios-Del Toro, E. E. & Cervantes, F. J. Anaerobic ammonium oxidation in marine environments: contribution to biogeochemical cycles and biotechnological developments for wastewater treatment. *Rev Environ Sci Biotechnol* **18**, 11–27 (2019).
65. Rappé, M. S., Connon, S. A., Vergin, K. L. & Giovannoni, S. J. Cultivation of the ubiquitous SAR11 marine bacterioplankton clade. *Nature* **418**, 630–633 (2002).
66. Kirchman, D. L. Growth Rates of Microbes in the Oceans. *Ann Rev Mar Sci* **8**, 285–309 (2016).
67. Becker, J. W., Hogle, S. L., Rosendo, K. & Chisholm, S. W. Co-culture and biogeography of Prochlorococcus and SAR11. *ISME J* **13**, 1506–1519 (2019).
68. Horak, R. E. A. *et al.* Ammonia oxidation kinetics and temperature sensitivity of a natural marine community dominated by Archaea. *ISME J* **7**, 2023–2033 (2013).
69. Tolar, B. B. *et al.* Contribution of ammonia oxidation to chemoautotrophy in Antarctic coastal waters. *ISME J* **10**, 2605–2619 (2016).
70. Wuchter, C. *et al.* Archaeal nitrification in the ocean. *Proceedings of the National Academy of Sciences* **103**, 12317–12322 (2006).
71. Lotti, T., Kleerebezem, R., Lubello, C. & van Loosdrecht, M. C. M. Physiological and kinetic characterization of a suspended cell anammox culture. *Water Res* **60**, 1–14 (2014).
72. Okabe, S., Kamigaito, A. & Kobayashi, K. Maintenance power requirements of anammox bacteria “Candidatus Brocadia sinica” and “Candidatus Scalindua sp.” *ISME J* **15**, 3566–3575 (2021).
73. Hatzenpichler, R. Diversity, physiology, and niche differentiation of ammonia-oxidizing archaea. *Appl Environ Microbiol* **78**, 7501–7510 (2012).

74. Wu, G., Zhang, T., Gu, M., Chen, Z. & Yin, Q. Review of characteristics of anammox bacteria and strategies for anammox start-up for sustainable wastewater resource management. *Water Science and Technology* **82**, 1742–1757 (2020).
75. White, A. E., Giovannoni, S. J., Zhao, Y., Vergin, K. & Carlson, C. A. Elemental content and stoichiometry of SAR11 chemoheterotrophic marine bacteria. *Limnol Oceanogr Lett* **4**, 44–51 (2019).
76. Almeida, J. S., Júlio, S. M., Reis, M. A. M. & Carrondo, M. J. T. Nitrite inhibition of denitrification by *Pseudomonas fluorescens*. *Biotechnol Bioeng* **46**, 194–201 (1995).
77. van den Berg, E. M., Boleij, M., Kuenen, J. G., Kleerebezem, R. & van Loosdrecht, M. C. M. DNRA and Denitrification Coexist over a Broad Range of Acetate/N-NO3− Ratios, in a Chemostat Enrichment Culture. *Front Microbiol* **7**, (2016).
78. Martens-Habbena, W., Berube, P. M., Urakawa, H., de la Torre, J. R. & Stahl, D. A. Ammonia oxidation kinetics determine niche separation of nitrifying Archaea and Bacteria. *Nature* **461**, 976–979 (2009).
79. Newell, S. E., Fawcett, S. E. & Ward, B. B. Depth distribution of ammonia oxidation rates and ammonia-oxidizer community composition in the Sargasso Sea. *Limnol Oceanogr* **58**, 1491–1500 (2013).
80. Zhang, Y. *et al.* Nitrifier adaptation to low energy flux controls inventory of reduced nitrogen in the dark ocean. *Proceedings of the National Academy of Sciences* **117**, 4823–4830 (2020).
81. Sun, X., Ji, Q., Jayakumar, A. & Ward, B. B. Dependence of nitrite oxidation on nitrite and oxygen in low□oxygen seawater. *Geophys Res Lett* **44**, 7883–7891 (2017).
82. Mdutyana, M. *et al.* Controls on nitrite oxidation in the upper Southern Ocean: insights from winter kinetics experiments in the Indian sector. *Biogeosciences* **19**, 3425–3444 (2022).
83. Awata, T. *et al.* Physiological Characterization of an Anaerobic Ammonium-Oxidizing Bacterium Belonging to the "Candidatus Scalindua" Group. *Appl Environ Microbiol* **79**, 4145–4148 (2013).
84. Letscher, R. T., Moore, J. K., Teng, Y.-C. & Primeau, F. Variable C□: N□: P stoichiometry of dissolved organic matter cycling in the Community Earth System Model. *Biogeosciences* **12**, 209–221 (2015).

Acknowledgments: We thank Clara Fuchsman for sharing data and Elena Litchman, Chris Klausmier and Alessandro Tagliabue for discussions. Simulations with the 3D ocean model were run on the Expanse system at the San Diego Supercomputer Center. The authors wish to acknowledge use of the Ferret program (http://ferret.pmel.noaa.gov/Ferret/), climate data operators (https://code.mpimet.mpg.de/projects/cdo/), NetCDF Operators (http://nco.sourceforge.net/), Python (www.python.org) and GIMP (https://www.gimp.org/) for the analysis and graphics in this paper.

Funding:

Simons Foundation postdoctoral fellowship in Marine Microbial Ecology (XS)

U.S. National Science Foundation grant OCE-1847687 (DM, DB)

Advanced Cyber infrastructure Coordination Ecosystem: Services and Support (ACCESS) program allocations TG-OCE170017 (DM, DB) and EES220053 (PJB, EZ),

which are supported by National Science Foundation grants 2138259, 2138286, 2138307, 2137603, and 2138296.

Author contributions: Each author's contribution(s) to the paper should be listed [we encourage you to follow the CRediT model]. Each CRediT role should have its own line, and there should not be any punctuation in the initials.

Examples:

Conceptualization: PJB, EZ

Methodology: PJB, EZ, JLW, DM

Software: PJB, EZ, DM, DB

Investigation: PJB, XS, EZ

Data acquisition: PJB, XS

Visualization: PJB

Funding acquisition: EZ, DB

Project administration: EZ

Supervision: EZ, DB

Writing – original draft: PJB, EZ

Writing – review & editing: PJB, XS, JLW, DM, DB, EZ

Competing interests: Authors declare that they have no competing interests.

Data and materials availability: All data and code are freely available. The chemostat model, model output, data, and scripts to reproduce the figures can be downloaded at https://doi.org/10.5281/zenodo.7653737. The code for the chemostat model is housed at https://github.com/pearseb/microbial_chemostat_model. The source code and the developments made to the ROMS-BEC2 ocean-biogeochemical ocean model is maintained at https://github.com/pearseb/BEC2-microbes.

Supplementary Materials

Materials and Methods

Supplementary Text

Figs. S1 to S9

Tables S1 to S6

References (*54–84*)

Movies S1 to S8

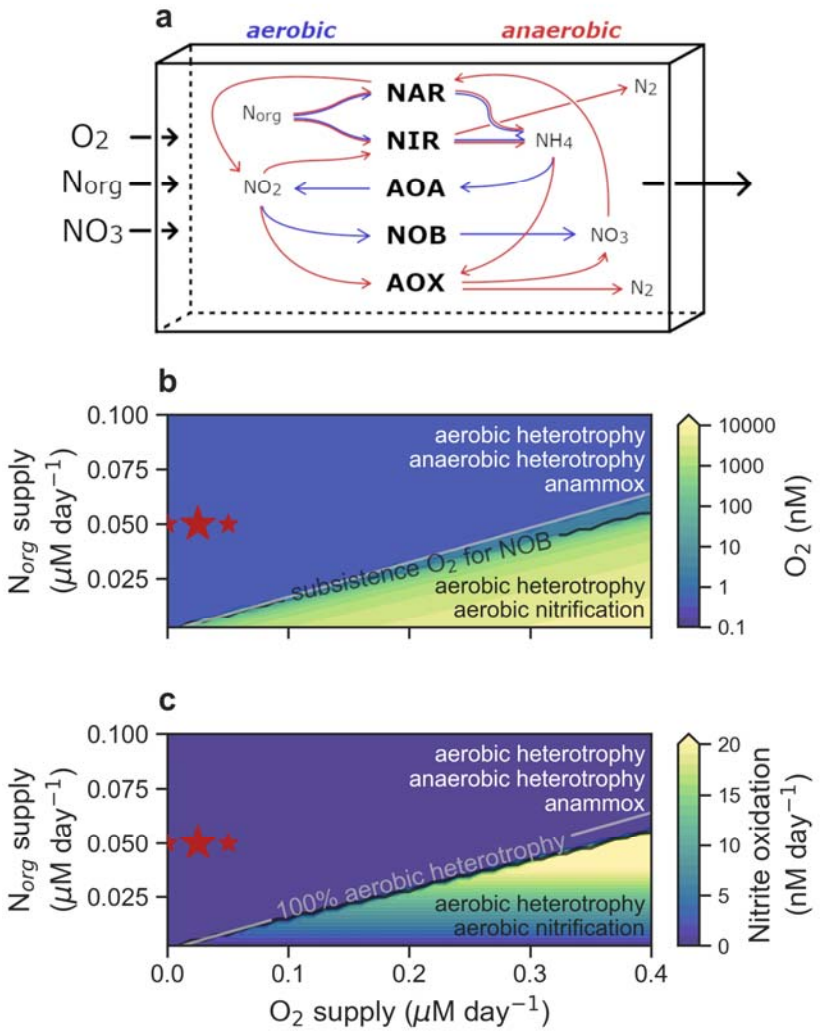

Fig. 1. Steady-state outcomes of the virtual chemostat model. (**A**), Schematic of the virtual chemostat model. The chemostat (single box model) contains aerobic (blue) and anaerobic (red) nitrogen cycling metabolisms carried about by key microbes: facultative nitrate- and nitrite-reducing heterotrophs (NAR and NIR), ammonia-oxidising archaea (AOA), nitrite-oxidising bacteria (NOB) and anammox bacteria (AOX). (**B**) Resulting steady-state oxygen concentration as a function of different rates of organic nitrogen (N_{org}) and O_2 supply. (**C**) Resulting rate of nitrite oxidation (nM day^{-1}). Silver contour is the point below which 100 % of heterotrophy is aerobic (Φ = 1, from Zakem et al. (***21***)). Black contour is the subsistence O_2 concentration for NOB (Table S3) indicating their competitive exclusion from the anoxic domain (i.e., where oxygen must be competed for). Resulting active metabolisms in the steady-state anoxic and oxic regimes are listed. The red stars indicate the range of background (constant) N_{org} and O_2 supply rates used as the background conditions in the O_2 pulse experiments (small red stars span the range of background supply rates while the large star indicates the supply rates results presented in Figure 2).

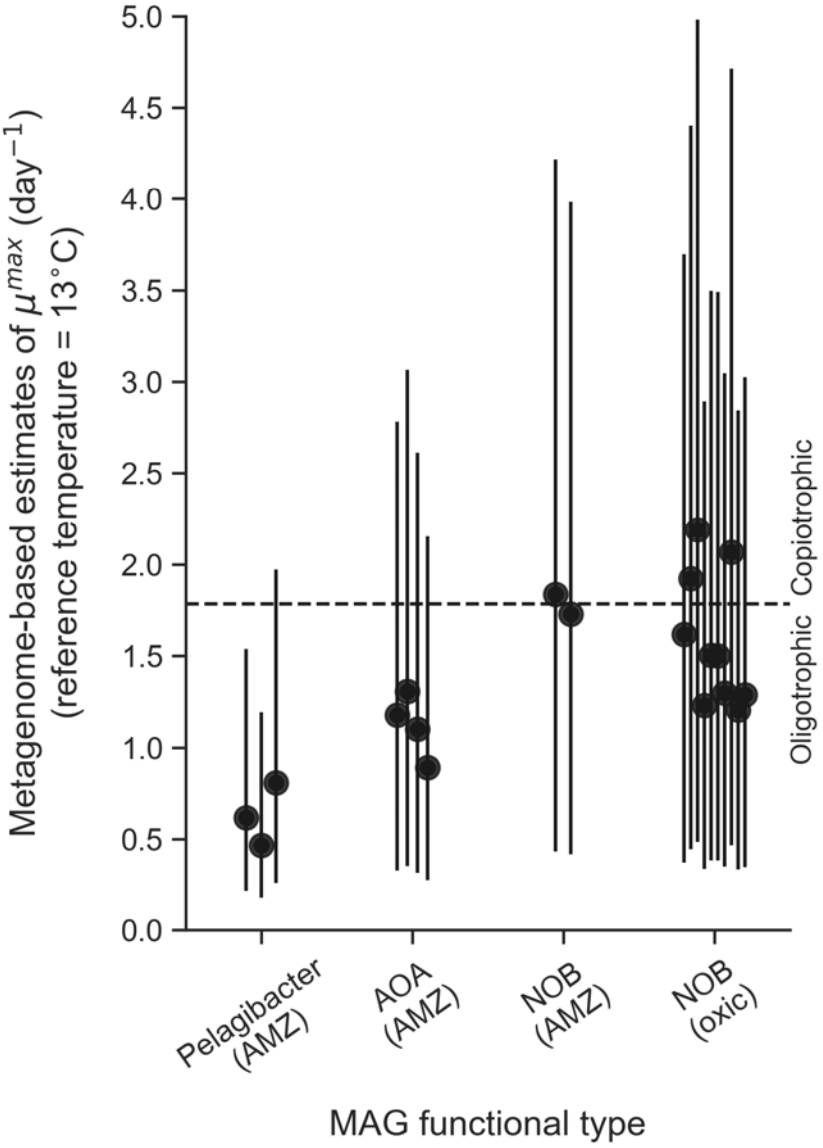

Fig. 2. Metagenome-based estimates of maximum growth rates of marine microbial functional types. Each dot is the central μ^{max} estimate for an individual metagenome-assembled genome (MAG) and the vertical lines are 95% confidence intervals. AMZ MAGs come from the East Tropical South Pacific **(*14*)**. NOB MAGs from oxic environments come from a range of environments (Table S4). μ^{max} was estimated using codon usage patterns **(*35*)** for a reference temperature of 13°C. The dashed line demarcates the threshold delineating 'oligotrophs' from 'copiotrophs' as well as the reliability of the estimates (higher for copiotrophs) according to previous analysis **(*35*)**.

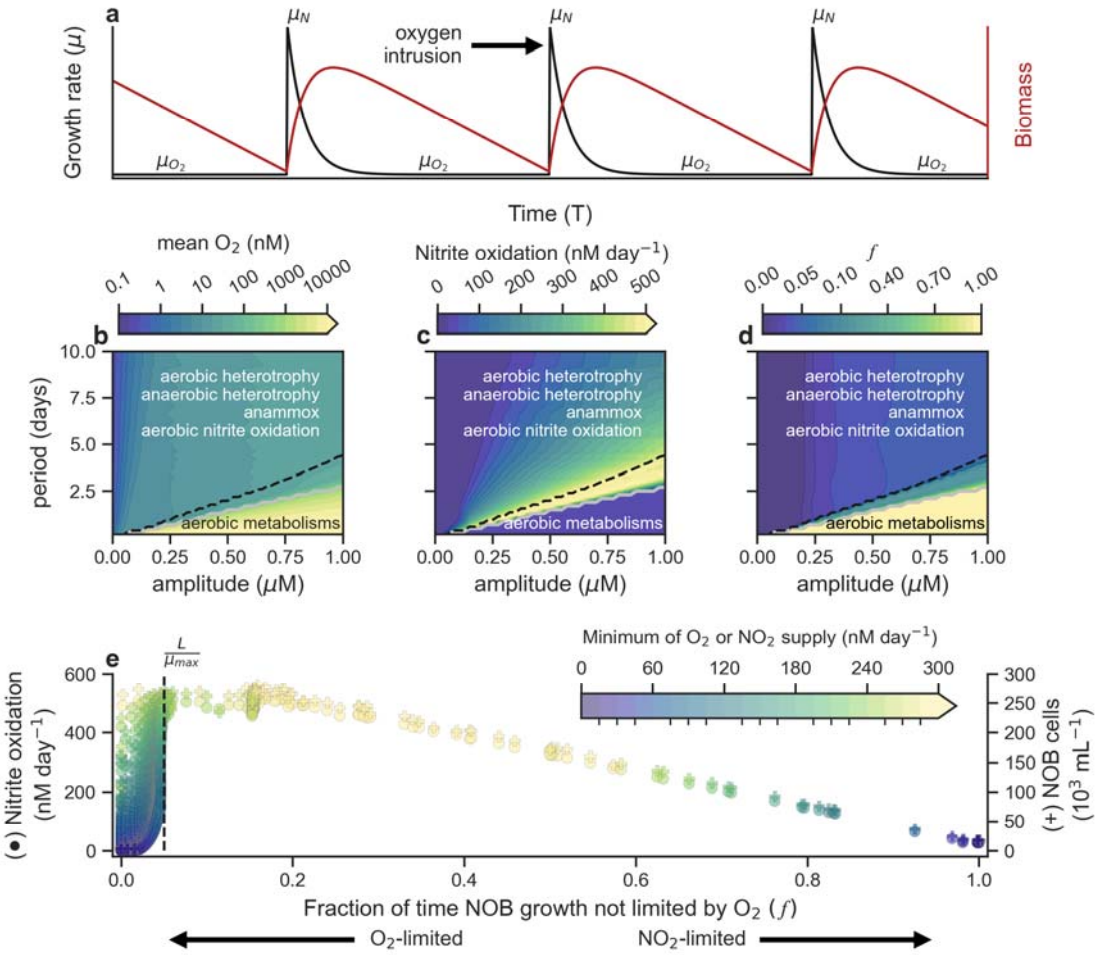

Fig. 3. Episodic oxygen pulses support aerobic nitrite oxidation in anoxic conditions. (**A**), Schematic illustrating how oxygen intrusions to an anoxic water parcel cause a shift from an oxygen-limited growth rate ( ) to a nitrogen-limited growth rate ( ) and rapid NOB biomass accumulation followed by loss after a return to (red). (**B**), Average concentration of dissolved oxygen (O_2; nM) over last 100 days of chemostat experiments (run to dynamic equilibrium) with background oxygen and organic matter supply of 0.025 and 0.050 µM day^{-1} (large red star in Fig. 1b,c). Silver line represents threshold where 100 % of heterotrophy becomes aerobic (**Φ** = 1, from Zakem et al. (***21***)). Active metabolisms in the anoxic and oxic regimes are listed. (**C**), Average rate of nitrite oxidation in nM day^{-1}. (**D**) Fraction of time NOB released from oxygen limitation ( ) in model. Black dashed line is analytically derived , where ——. (**E**), Relationship between , the rate of nitrite oxidation (circles) and NOB abundance (pluses); assumes NOB contain 39.8 fg C per cell (***45***). Points are colored by the average rate of oxygen or nitrite supply, whichever is lowest (nM day^{-1}). Black dashed line is the analytically derived for NOB (Eqn. 3).

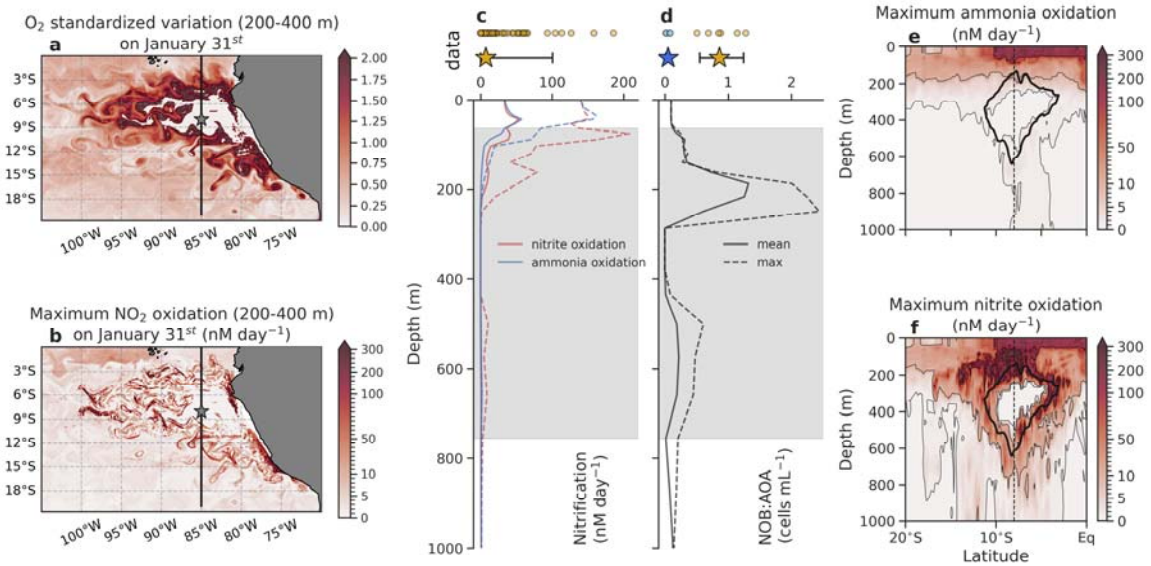

Fig. 4. AMZ nitrite oxidation in an eddy-resolving 3D ocean model. (**A**), Standardized variation (standard deviation divided by mean) in oxygen between 200 and 400 metres depth. (**B**), Maximum rate of nitrite oxidation between 200 and 400 meters depth. (**C**), Average (solid lines) and maximum (dashed lines) annual rates of ammonia oxidation (blue) and nitrite oxidation (red) at location denoted by the grey star marker in (**A**,**B**). Grey shading denotes AMZ where $O_2 < 1$ µM. (**D**), Average (solid line) and maximum (dashed line) ratio of NOB to AOA biomass at location denoted by the star marker in (**A**,**B**). Biomass as output by the model is converted to cells per mL assuming 39.8 fg carbon per cell of NOB and 11.5 fg carbon per cell of AOA (Methods) (*45*). Observed nitrite oxidation rates within low-oxygen waters (gold circles) in locations across the East Pacific (*12*, *16*) are shown above the plot in (**C**). Observed NOB:AOA in the data above the plot in (**B**) are counts of genes encoding nitrite oxidoreductase (Nxr) to ammonia monooxygenase (amoA) (*17*), assuming that there are 4 copies of Nxr per NOB cell. Blue markers are from oxygenated waters. Gold markers are from the AMZ. Dots are individual observed values, while the star and error bars below show the median and 5th to 95th percentile spread. Annual maximum value of ammonia oxidation (**E**) and nitrite oxidation (**F**) along the transect (black line in panels (**A**,**B**). Figure generated from daily averages over one year.

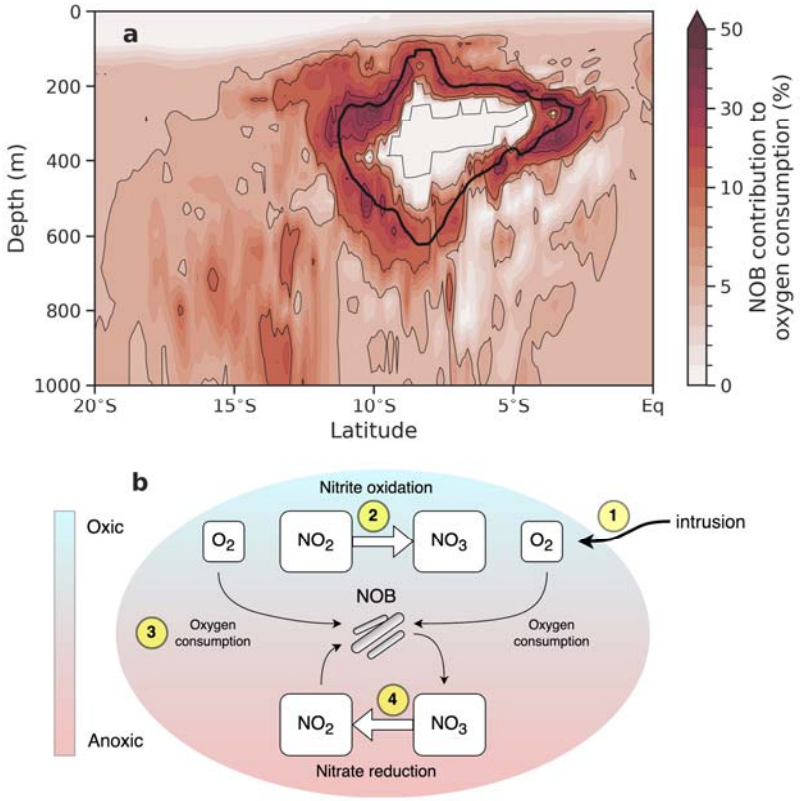

Fig. 5. The stabilizing biological feedback of NOB in response to oxygen intrusions. (**A**), Annual average contribution of NOB to oxygen consumption. The AMZ is defined as where oxygen < 1 µM. (**B**), Intrusions (1) stimulate nitrite oxidation (2) and gains in NOB biomass, which in turn elevates oxygen consumption (3) and a more rapid return to anoxia, thereby supporting production of nitrite via anaerobic nitrate reduction (4), which maintains the ability to buffer oxygen intrusions.